HHS Public Access

Author manuscript

ACS Chem Neurosci. Author manuscript; available in PMC 2016 August 19.

Published in final edited form as:

ACS Chem Neurosci. 2015 August 19; 6(8): 1476–1485. doi:10.1021/acschemneuro.5b00134.

Targeting the Cyclophilin Domain of Ran-binding Protein 2 (Ranbp2) with Novel Small Molecules to Control the Proteostasis of STAT3, hnRNPA2B1 and M-Opsin

Kyoung-in Cho[1], **Andrew Orry**[2], **Se Eun Park**[1], and **Paulo A. Ferreira**[1,3,#]

[1]Department of Ophthalmology, Duke University Medical Center, Durham, NC 27710

[2]MolSoft LLC, San Diego, CA 92121

[3]Department of Pathology, Duke University Medical Center, Durham, NC 27710

Abstract

Cyclophilins are peptidyl *cis-trans* prolyl isomerases (PPIases), whose activity is typically inhibited by cyclosporine A (CsA), a potent immunosuppressor. Cyclophilins are also chaperones. Emerging evidence supports that cyclophilins present non-overlapping PPIase and chaperone activities. The proteostasis of the disease-relevant substrates, signal transducer and activator of transcription 3 and 5 (STAT3/STAT5), heterogeneous nuclear ribonucleoprotein A2B1 (hnRNPA2B1) and M-opsin, are regulated by non-overlapping chaperone and PPIase activities of the cyclophilin domain (CY) of Ranbp2, a multifunctional and modular scaffold which controls nucleocytoplasmic shuttling and proteostasis of selective substrates. Although highly homologous, CY and the archetypal cyclophilin A (CyPA) present distinct catalytic and CsA-binding activities owing to unique structural features between these cylophilins. We explored structural idiosyncrasies between CY and CyPA to screen *in silico* nearly 9 million small molecules (SM) against the CY PPIase pocket and identify SMs with selective bioactivity toward STAT3, hnRNPA2B1 and/or M-opsin proteostasis. We found three classes of SMs that enhance the cytokine-stimulated transcriptional activity of STAT3 without changing latent and activated STAT3 levels, down-regulate hnRNPA2B1 or M-opsin proteostasis, or a combination of these. Further, a SM which suppresses hnRNPA2B1 proteostasis also inhibits strongly and selectively the PPIase activity of CY. This study unravels chemical probes for multimodal regulation of CY of Ranbp2 and its substrates and this regulation likely results in the allosterism stemming from the interconversion of conformational substates of cyclophilins. The results also demonstrate the feasibility of CY in drug discovery against disease-relevant substrates controlled by Ranbp2 and they open new opportunities for therapeutic interventions.

Keywords

Ran-binding protein 2 (Ranbp2); cyclophilin; chaperone; proteostasis; RNPA2B1; STAT3; M-opsin; chemical ligands

[#]To whom correspondence should be addressed: Paulo A. Ferreira, Duke University Medical Center, DUEC 3802, 2351 Erwin Road, Durham, NC 27710, Tel. 919-684-8457; Fax: 919-684-3826; paulo.ferreira@duke.edu.

INTRODUCTION

Cyclophilins are members of peptidyl *cis-trans* prolyl isomerases (PPIases),[1–3] whose activity promotes protein folding or conformational switches in protein signaling.[4–6] Cyclophilins bind also the cyclic undecapeptide and potent immunosupressor drug, CsA.[7–9] Cyclophilin A (CyPA or PPIA), a prototypical member of cyclophilin family, mediates immunosuppression[9,10] and non-immunosuppressor structural variants of CsA have been exploited in the treatment of diseases,[9,11,12] such as infections caused by HIV-1 and HCV.[13–18]

Cyclophilins act also as chaperones. For example, the cyclophilin encoded by *ninaA* of *Drosophila* chaperones the biogenesis of selective opsins of photoreceptor neurons.[19–21] The molecular bases of the chaperone activity of NinaA and other cyclophilins remain unclear; however, mutational or structural studies of ninaA,[5] CyPH/PPIL1[22–24] or CyPB (PPIB)[25] support this activity arises from the stable association of substrates to binding sites in cyclophilin that do not overlap with its PPIase site and that are not affected by CsA binding. This notion of mutually exclusive sites in cyclophilins toward distinct substrates was strengthened by the findings that cyclophilin domain (CY) of Ranbp2 harbors selective physiological activities towards four disease-relevant substrates, STAT3/STAT5, hnRNPA2B1 and M-opsin.[26] Ranbp2 is a large 358 kDa multimodular, pleiotropic and cytoplasmic peripheral nucleoporin, which is not exclusively localized at nuclear pores.[26–31] Selective domains of Ranbp2 control nucleocytoplasmic trafficking,[28,31–37] sumoylation,[38–40] microtubule-based motor activity of kinesin-1[41–43] and proteostasis of selective proteins.[26,44–47] In particular, M-opsin biogenesis is dependent on the C-terminal chaperone activity of CY, but not on CY PPIase activity.[26] By contrast, loss of CY PPIase activity down-regulates the proteostasis of hnRNPA2B1, whereas impairments of CY PPIase and C-terminal chaperone activities lack apparently untoward effects of CY association with latent and stress-activated STAT3/STAT5.[26] Regulation of proteostasis of substrates by CY activities is important, because STAT3/STAT5 misregulation is linked to inflammation, cancer and neurodegeneration,[48–55] aggregation-prone mutations in *hnRNPA2B1* cause multisystem proteinopathies and amyotrophic lateral sclerosis (ALS)[56] and those in L/M-opsins (*OPN1LW*/*OPN1MW*) lead to cone photoreceptor neuron dystrophy and color blindness.[57] Mounting evidence also support that HIV-1 usurps the PPIase activity of CY of Ranbp2. The binding and prolyl isomerization of the CyPA-binding loop of HIV-1 capsid to CY of Ranbp2 uncoats and promotes nuclear entry of HIV-1.[15,58]

Recent data support that the archetypal CyPA undergoes conformational fluctuations leading to side-chain conformational heterogeneity in residues unrelated and related to catalysis.[3, 59–61] For example, alternative side-chain rotamers, such as Phe113 at the base of the PPIase pocket, can cause long-range chemical shifts.[59] These critical data establish a direct relationship between rates of conformational substates of CyPA and catalysis. The dynamic properties of CyPA are likely extended to other cyclophilin members, such as CY of Ranbp2. For example, CY can undergo phosphorylation of residues away from the PPIase site and this modification reduces the PPIase activity of CY.[26] Collectively, these data support that cyclophilins interconvert between conformational substates and that distinct structural ensembles of cyclophilins are coupled directly to unique function(s). Importantly,

these mechanisms may be explored to modulate pharmacologically and selectively manifold activities of cyclophilins on their substrates.

Here, we explored the heterogeneity of structural ensembles between the PPIase pockets of CY of Ranbp2 and its closest homolog, CyPA, to screen nearly 9 million small molecules and discover unique chemical probes selective to CY and that modulate distinct features of proteostasis of CY substrates, STAT3, hnRNPA2B1 and M-opsin.

RESULTS AND DISCUSSION

Exploring the structural heterogeneity of CY and CyPA for *in silico* screening of chemical ligands of CY

The primary sequence of CY of Ranbp2 is 65% identical to CyPA (Figure 1a).[29] Comparison between the available PDB crystal structures of the PPIase pockets of CY and CyPA indicates that CY harbors an extended PPIase pocket with an area and volume of 370Å^2 and 357Å^3 compared to 301 Å^2 and 312Å^3 of CyPA, respectively (Figure 1b). Further, several critical residues within or surrounding the PPIase pocket were unique to CY of Ranbp2. For example, A103 and W121 in CyPA are replaced by Q3163 and H3181 in CY of Ranbp2, respectively (Figure 1c). These highly conserved residues among cyclophilins[29] are critical to CsA binding to CyPA. Q3163 is predicted to restrict binding of CsA to CY, whereas the mutations, W121F and W121A, in CyPA were shown to decrease 75 and 200-fold their binding activities to CsA and 2- and 13-fold their catalytic efficiencies (k_{cat}/K_m), respectively.[62] Conversely, replacement of the equivalent residue H141W of CyP40 increases its catalytic efficiency and binding to CsA.[63] Hence, the non-conserved Q3163 and H3181 in CY of Ranbp2 are thought to contribute to its decreased catalytic efficiency on standard peptidyl-prolyl substrates and CsA-binding activity.[26,29] In addition to other conservative and non-conservative substitutions in CY PPIase pocket (Figure 1c), CyPA and CY present also surface electrostatic changes owing to differences of orientation of side chains of conserved lysines towards or away the PPIase pocket (e.g. K3142 (K82 in CyPA) and K3185 (K125 in CyPA)) (Figures 1c and d) and whose acetylation in CyPA promotes surface electrostatic shifts and PPIase inhibition.[64,65]

We took advantage of the structure of CY determined at 1.75 Å (PDB 4I9Y)[64] and unique structural ensembles between the PPIase pockets of CY and CyPA (PDB 2CPL)[66] (Figure 1c) to screen a library of nearly 9 million small molecules against the extended CY PPIase pocket with structure-based and virtual ligand screening (VLS) approaches (Figure 2). These approaches produced 679 potential ligands to the PPIase pocket of CY of Ranbp2 after counter-screening ligand candidates of CY against the PPIase pocket of CyPA (Figure 2). Fourteen high-scoring compounds against the atomic structure of CY determined at 1.75 Å (PDB 4I9Y) were selected for experimental analysis upon visual inspection of various structural features, such as geometries, functional groups, and interactions with the receptor. Figure 3 shows the chemical structures of six of the fourteen candidate ligands of CY and that were found in this study to show pharmacological activity toward physiological substrates of CY of Ranbp2. Compounds without CY pharmacological activity likely represent false positives from the *in silico* screening owing to the lack of the incorporation of dynamics of CY and absence of multiple atomic structures of CY.

Modulation of STAT3-transcriptional activity by chemical ligands of CY

Chemical compounds were assessed for their ability to modulate STAT3 transcriptional activity. We chose a STAT3 luciferase reporter HeLa stable cell line to screen the compounds, because this cell line lacks endogenous activated STAT3 in the absence of the cytokine, oncostatin-M (OncM), but robust STAT3 activation (STAT3(P)) ensues upon OncM stimulation (Figures 4a and b). By contrast, IL-6 had no effect on STAT3-transcriptional activity (Figure 4b). Further, this line expresses endogenously hnRNPA2B1 and Ranbp2, whose levels remain unchanged by the absence or presence of OncM (Figure 4a).

We examined the dose-response of STAT3-transcriptional activation in the presence of increasing concentrations of chemical compounds. As shown in figure 4c, we found that four chemicals, compound 1, 2, 10 and 11, enhanced STAT3-transcriptional activity and among these, compound 10 had the strongest effect (> 2-fold increase). By contrast, compound 3 (Figure 4c) and other compounds had no effect (data not shown). Interestingly, compound 1 was extremely labile because its bioactivity was completely lost upon solvation and short-term storage. Conversely, compound 14 was cytotoxic and was not included for further analysis. Finally, the enhancement of STAT3-transcriptional activity was not caused by changes in the levels of latent and activated STAT3, because the levels of STAT3 and STAT3(P) were unchanged in the absence and presence of the compounds with and without effects on STAT3-transcriptional activity (Figure 4d).

CyPA and CyPB bind to CsA and this association promotes the down-regulation of STAT3-transcriptional activity.[67] To probe the selectivity of the mechanisms of regulation of STAT3-transcriptional activation, we treated cells with CsA in the absence and presence of OncM. In comparison to unchallenged HeLa cells, CsA had no effect on STAT3 activation. However, CsA reduced by ~50% the levels of STAT3-transcriptional activity upon treatment of cells with OncM (Figure 4e). Hence, CsA and compounds 1, 2, 10 and 11 elicit contrasting effects in STAT3-transcriptional activation.

Modulation of hnRNPA2B1 proteostasis by chemical ligands of CY

To assess the effect of the chemical compounds towards CY in hnRNPA2B1 proteostasis, the STAT3 luciferase reporter HeLa stable cell line was cultured without cytokine challenge in the absence and presence of the compounds. As shown in figure 5a (upper panel), compounds 11–13 elicited strong down-regulation of hnRNPA2B1 levels. Quantitative analyses of immunoblots showed that compounds 11–13 elicited a greater than 2-fold reduction of hnRNPA2B1 levels, whereas compounds 1 and 10, and all other compounds, had milder and no effects in hnRNPA2B1 proteostasis, respectively (Figure 5a, lower panel). Finally, there was also a dose-dependent response of hnRNPA2B1 down-regulation towards compound 11 (Figure 5b).

Modulation of M-opsin by chemical ligands of CY

We used a transformed cone photoreceptor line, which expresses endogenously M-opsin,[68,69] to ascertain the effect in M-opsin proteostasis of compounds without overlapping effects in STAT3-transcriptional activation and regulation of hnRNPA2B1 proteostasis,

such as compounds 2 and 13. As shown in figure 5c, compounds 2 and 13 exerted mild, but contrasting and significant effects, in M-opsin proteostasis. Compound 2 and 13 selectively decreased and increased M-opsin levels, respectively.

Inhibition of CY PPIase activity by chemical compounds

CY of Ranbp2 harbors non-overlapping PPIase and chaperone activities towards STAT3/STAT5, hnRNPA2B1 and M-opsin, and CY likely undergoes conformational substates with inherent effects on CY functions and PPIase activity.[26] To discern further the mechanisms of compounds 1–13 in CY functions, we measured the direct effects of these compounds on CY PPIase activity. Among these compounds, only compound 13 had a potent and selective inhibitory effect on CY PPIase activity. As shown in figure 6a, the IC_{50} of compound 13 for CY of Ranbp2 was $\simeq 4\times10^{-13}$ M. In addition, we evaluated the selectivity of compound 13 and CsA toward the PPIase activities of CyPA and CY at known saturating PPIase inhibitory concentrations of compound 13 (this study, Figure 6a) and CsA for CY and CyPA, respectively.[62,65] As shown in figure 6b, 100 nM of CsA inhibited strongly the PPIase activity of CyPA but had no effect on CY PPIase activity. By contrast, compound 13 did not inhibit the PPIase activity of CyPA. Hence, compound 13 is a novel, potent and highly selective orthosteric inhibitor of the PPIase activity of CY of Ranbp2.

Distinctive features of CY-ligand complexes

To gain insights to the structural bases for the pharmacological and biochemical effects between the compounds described in this study, we examined the poses of the ligands docked in the extended PPIase pocket of Ranbp2. We modeled and calculated all the contact areas between the residues of CY and functional groups of ligands and compared these to the crystal structure of CyPA-CsA complex (PBD 1CWA).[70] As shown in figure 7a, compound 11, which presents dual activities for STAT3 and hnRNPA2B1, is predicted to interact with highest number of residues (seven) which do not interact with CsA in CyPA. Compounds 10 and 11 share pharmacological properties and sixteen interacting residues. Among these residues, five do not interact with CsA in CyPA and three (D3131, Q3163 and N3169) are not conserved in CyPA. Strikingly, compound 13, which suppresses CY PPIase activity, is the only compound that is predicted to establish hydrogen bonds with the highly conserved residues, R3115 (R55 in CyPA) and H3186, whereas a single hydrogen bond is established between all other compounds and R3115 (Figure 7b). Finally, compound 11 has an extended configuration compared to all other compounds by protruding out of the PPIase pocket toward D3141, K3142 and N3169 (Figure 7c).

Conclusions

This study identified the first known chemical ligands with relative potency and selectivity toward CY of Ranbp2 and with idiosyncratic activities toward the modulation of the proteostasis of physiological substrates of CY, such as STAT3, hnRNPA2B1 and M-opsin. Specifically, this study found compound 2 enhances STAT3-transcriptional activation without affecting hnRNPA2B1 proteostasis, whereas compounds 12 and 13 down-regulate hnRNPA2B1 proteostasis without affecting STAT3-transcriptional activation. Further, compound 2 and 13 promote also mild down-regulation and up-regulation of M-opsin proteostasis, respectively. No chemical enhancers of STAT3 activity are known to this

date.[48] Likewise, chemical regulators of hnRNPA2B1 and M-opsin proteostasis are elusive. Regulation of STAT3 activity is important in clinical conditions, such as cancer and neurodegeneration promoted by intrinsic and extrinsic pathological stressors and in which activated STAT3 is thought to act as an early prosurvival factor.[48–54,71] A potential concern is whether an enhancement of prosurvival responses caused by activated STAT3 alone promotes oncogenesis in neurodegenerative therapies. However, this concern is mitigated by recent data supporting that therapeutic augmentation by activated STAT3 promotes photoreceptor survival and delays degeneration of photoreceptors across various inherited models of photoreceptor dystrophies and without apparent transformation of retinal neurons.[55] Hence, pharmacological enhancers of STAT3 activity may boost the prosurvival potential of STAT3 across multiple neurodegenerative conditions. On the other hand, human mutations in prion-like domains of hnRNPA2B1 cause MSP and ALS,[56] whereas mutations in M-opsin compromise cone photoreceptor neural function and promote color blindness.[57] These mutations are thought to promote the misfolding and/or aggregation of cytotoxic hnRNPA2B1 and opsin conformers.[56,72] In this regard, this study opens new venues for the pharmacological down-regulation of disease-relevant substrates when pathological accumulations or aggregation of conformational and kinetically trapped folded substrates compromise neural survival. Finally, emerging data also support that hnRNPA2B1 is a driving oncogene in glioblastoma and that hnRNPA2B1 knockdown is accompanied by a reduction of activated STAT3 and transformation potential.[73,74] Hence, the chemical compounds herein uncovered may have therapeutic applications in other diseases, such as glioblastomas with over-expression of hnRNPA2B1.

This study also shows that the regulation of chaperone and PPIase activities of cyclophilins may undergo a higher level of complexity than hitherto appreciated. Our prior work showed that the mutation, R3115A (R55 in CyPA), which causes the loss of PPIase activity of CY, led to the selective post-transcriptional down-regulation of hnRNPA2B1, without apparently affecting STAT3 proteostasis.[26] By contrast, this study shows that compound 13, which selectively inhibits also the PPIase of CY and down-regulates hnRNPA2B1, shares similar pharmacological properties with compounds 10–12 which have no inhibitory effect on CY PPIase activity. Assuming that these compounds maintain similar bioactive conformations *in vitro* and *in vivo*, the data indicate that loss of PPIase activity alone may not account for the down-regulation of hnRNPA2B1. Further, compound 13 is predicted to be anchored by hydrogen bonding to highly conserved residues among cyclophilins, such as H3186 (H126 in CyPA) and the catalytic residue R3115A (R55 in CyPA). Hence, it is likely that unique interactions of shared and unique residues of CY with compounds 10–13, but not CsA, may contribute significantly to their unique pharmacological properties and that CY presents allosteric coupling of PPIase and chaperone activities. This ligand-elicited allosterism at the PPIase pocket may promote long-range chemical shifts in CY and the generation of CY conformers with distinct chaperone propensities toward STAT3, hnRNPA2B1 and M-opsin. Ultimately, X-ray crystal structures of chemical ligand-CY complexes, ligand structure-activity relationships and chemical-genetic complementation studies are needed to gain additional insights into the mechanisms underpinning the pharmacological regulation of CY by the novel aforementioned compounds.

Another surprising observation was that we did not observe changes in latent and activated STAT3 levels by compounds that enhance STAT3-transcriptional activation and that compound 13 with CY PPIase inhibitory activity had no effect on STAT3-transcriptional activation. Although these pharmacological and prior results support a lack of physiological effects of *cis-trans* prolyl isomerization in STAT3 proteostasis and STAT3 association to Ranbp2,[26] they suggest a model whereby CY chaperones and boosts the *trans*-activation potential of STAT3 by sampling dynamic conformational substates of activated STAT3 and shifting the equilibrium between these substates to favor the formation of STAT3 conformer(s) with high *trans*-activation potential or nuclear translocation efficiencies.

Pharmacological regulation of protein-protein interactions are often viewed as difficult to target owing to large and flat interfaces between interacting partners.[75] However, small molecule-mediated allosteric (induced-fit) regulation of protein interacting interfaces may produce dynamic shifts in pre-existing and nearly isoenergetic ground conformational substates that are linked to distinct functional properties of a protein. This concept was introduced first by Linderstrøm-Lang and Schellman[76] and extended by Monod *et al* to multisubunit proteins[77] and more recently to "single-domain" proteins,[78–80] including cyclophilins.[59,61] We suggest that the dynamic interconversion of functionally and structurally distinct ensembles may not only underlie chaperone activity through the adaptive recognition of client proteins, but have also critical implications to the allosteric regulation of bidirectional transport of substrates through the nuclear pore. Oscillations in conformational substates of CY (and other domains)[43] of Ranbp2 and exclusive association of selective conformers to import (e.g. STAT3) or export substrates (e.g. hnRNPA2B1) may contribute to the directionality of nucleocytoplasmic trafficking and protestasis of client proteins. In this regard, the chemical probes here discovered will help to explore pharmacologically the dynamic roles of protein conformational substates in the regulation of nucleocytoplasmic trafficking, recognition and proteostasis of client proteins which likely extend beyond those examined in this study, such as the capsid of HIV-1.[15,58]

METHODS

Virtual Ligand Screening (VLS) of MolCart database

The 1.75 Å resolution crystal structure of human CY of RANBP2 (PDB code 4I9Y) was used in the virtual screen.[64] The structure was prepared for virtual screening by using standard protocols in Internal Coordinate Mechanics (ICM-Pro) software v3.8 (MolSoft's LLC, San Diego, CA).[81–83]

The MolCart Compounds database (http://www.molsoft.com/molcart-compounds.html) containing 8,932,994 commercially available chemicals was filtered using a relaxed set of "Lipinski-like" chemical drug-like property rules.[84] The database was then screened against the extended orthosteric PPIase pocket of CY of RanBP2. VLS was performed with Internal Coordinate Mechanics-Pro (ICM-Pro VLS software v3.8) and dockScan v.4.41 (MolSoft's LLC, San Diego, CA). The ICM program performs global optimization of the entire flexible ligand in the receptor field and combines large-scale random moves of several types with gradient local minimization and a search history mechanism using the ICM biased probability Monte Carlo procedure.[81] Docking poses were evaluated according to the

weighted components of the ICM-VLS scoring function,[85] which gives a good approximation of the binding free energy between a ligand and a receptor and is a function of different energy terms based on a force-field. The side-chains of CY were not explicitly flexible during the screening. A soft van der Waals potential was used to allow partial flexibility between the ligand and receptor but no large side-chain or backbone movements were incorporated. Based on the distribution of scores a scoring threshold of −37 was employed to differentiate potential binders from non-binders. The ranked hit list was checked for compounds with unusual chemical properties (e.g. reactive or potentially PAIN compounds[86]) and high strain (e.g. *cis* amides) and these chemicals were removed. The hit list was then clustered using MolSoft's Atomic Property Field (APF) method[87] to select a diverse set of 735 chemicals for experimental testing.

The hit list was then counter-screened against the active site of CyPA\PPIA (PDB 2CPL).[66] Fifty six of the chemicals in the final ranked hit list of CY of Ranbp2 were predicted to bind to CY of RanBP2 and CyPA and they were removed from the final hit list. Top scoring compounds were visually inspected and 14 compounds were selected for experimental evaluation.

Reagents and antibodies

Oncostatin-M (OncM) and interleukin 6 (IL6) (R&D Systems); monoclonal mouse mAb414 against Nup358/Ranbp2, Nup153 and Nup 62 (Convance, Emeryville, CA); rabbit anti L/M opsin no. 21069;[42] rabbit polyclonal anti-hnRNPA2B1 (Proteintech, Chicago, IL); rabbit monoclonal anti-STAT3 (Cell Signaling, Boston, MA); rabbit anti-pSTAT3 (Cell Signaling); mouse rabbit anti-glyceraldehyde 3-phosphate dehydrogenase (Gapdh) (Santa Cruz Biotechnology), rabbit anti-hsc70 (Enzo Life Science, Farmingdale, NY); bovine thymus cyclophilin A (Sigma); Suc-ALPF-*p*NA (Bachem Bioscience); cyclosporine A (CsA, Sigma); bovine pancreas α-chymotrypsin type 1-S (Sigma). Purity of chemical compounds no. 1, 2, 10, 11, 12 and 13 were 93, 100, 94, 98, 92 and 96%, respectively, as provided by the manufacturers.

Cell culture

The STAT3 luciferase reporter HeLa stable cell line (Signosis, Santa Clara, CA) was maintained in DMEM (Invitrogen) supplemented with serum inactivated fetal bovine serum (Hyclone), penicillin and streptomycin. HeLa cells were seeded in 96-well plates (8,000 cells per well) and cultured overnight at 37°C in the presence of 5% CO_2 and 100% humidity. For STAT3 activation and small compound screenings, HeLA cells were then challenged for 16 hours with OncM or IL-6 in 0.1% FBS and in the presence or absence of various concentrations of small compounds or CsA dissolved in anhydrous DMSO. DMSO concentration between treatments with and without compounds was kept constant. Then, luciferase assays were carried out as recommended by the manufacturer (Luciferase reporter system, Promega). Luminescence was measured with a SpectraMax M5 spectrometer plate reader (Molecular Devices). For analysis of hnRNPA2B1 and M-opsin proteostasis, HeLa cells and the murine photoreceptor cell line, 661W,[68,69] underwent the same procedures with the exception that they were grown to confluency (~1.2 million cells) in 6-well plates without cytokine stimulation and in the absence or presence of small compounds. Viability

and cytotoxicity were assessed with ApoTox-Glo Triplex Assay (Promega), microscopic examination, and comparisons between small molecules at 250 μM and staurosporin at 5 μM. Cells were harvested and lysed in RIPA buffer.

PPIase assays

Recombinant CY of Ranbp2 was purified as described elsewhere.[26,88] PPIase assays for the *cis-trans* prolyl isomerization of Suc-ALPF-*p*NA by recombinant CY of Ranbp2 (50 nM) or thymus-purified CyPA (5 nM) were performed using the chymotrypsin-coupled assay exactly as described previously, but in the absence or presence of small compounds or CsA.[26,29] The first-order rate constants, k, and catalytic efficiency, k_{cat}/K_m, were determined with Origin software v8.5. (Northampton, MA) and exactly as described previously.[26,29] IC_{50} value for CY PPIase inhibitor(s) (small compound) was ascertained using the chymotrypsin-coupled assay described above.

Quantitative immunoblots analyses

RIPA-solubilized cell homogenates were resolved in standard Hoefer (Holliston, MA) or premade 4–14% Criterion (BioRad) SDS-polyacrylamide gels. Changes in protein levels caused by compound treatments were ascertained by immunoblots and densitometric analyses as described previously.[26] Blots were reprobed for housekeeping proteins. Band intensities were quantified Metamorph v 7.0 (Molecular Devices) and integrated density values (idv) of representative bands were normalized to the background and idv of Gapdh or hsc70. Data were analyzed by the two-tail *t*-test and a p value of ≤0.05 was considered significant.

Acknowledgments

We thank the undergraduate summer fellows Aitana Zermeno (Howard Hughes Research Fellows Program, Duke University) and Basirul Haque (North Carolina State University) for their help with these studies.

FUNDING SOURCES. This work was supported by the National Institutes of Health grants EY019492 and GM083165 to PAF.

References

1. Fischer G, Wittmann-Liebold B, Lang K, Kiefhaber T, Schmid FX. Cyclophilin and peptidyl-prolyl cis-trans isomerase are probably identical proteins. Nature. 1989; 337:476–478. [PubMed: 2492638]
2. Takahashi N, Hayano T, Suzuki M. Peptidyl-prolyl cis-trans isomerase is the cyclosporin A-binding protein cyclophilin. Nature. 1989; 337:473–475. [PubMed: 2644542]
3. Camilloni C, Sahakyan AB, Holliday MJ, Isern NG, Zhang F, Eisenmesser EZ, Vendruscolo M. Cyclophilin A catalyzes proline isomerization by an electrostatic handle mechanism. Proc Natl Acad Sci U S A. 2014; 111:10203–10208. [PubMed: 24982184]
4. Schiene-Fischer C, Aumuller T, Fischer G. Peptide Bond cis/trans Isomerases: A Biocatalysis Perspective of Conformational Dynamics in Proteins. Top Curr Chem. 2011
5. Ferreira PA, Orry A. From Drosophila to humans: reflections on the roles of the prolyl isomerases and chaperones, cyclophilins, in cell function and disease. J Neurogenet. 2012; 26:132–143. [PubMed: 22332926]
6. Lu KP, Finn G, Lee TH, Nicholson LK. Prolyl cis-trans isomerization as a molecular timer. Nat Chem Biol. 2007; 3:619–629. [PubMed: 17876319]

7. Handschumacher RE, Harding MW, Rice J, Drugge RJ, Speicher DW. Cyclophilin: a specific cytosolic binding protein for cyclosporin A. Science. 1984; 226:544–547. [PubMed: 6238408]
8. Colgan J, Asmal M, Yu B, Luban J. Cyclophilin A-deficient mice are resistant to immunosuppression by cyclosporine. J Immunol. 2005; 174:6030–6038. [PubMed: 15879096]
9. Galat A, Bua J. Molecular aspects of cyclophilins mediating therapeutic actions of their ligands. Cell Mol Life Sci. 2010; 67:3467–3488. [PubMed: 20602248]
10. Schreiber SL. Chemistry and biology of the immunophilins and their immunosuppressive ligands. Science. 1991; 251:283–287. [PubMed: 1702904]
11. Edlich F, Fischer G. Pharmacological targeting of catalyzed protein folding: the example of peptide bond cis/trans isomerases. Handb Exp Pharmacol. 2006:359–404. [PubMed: 16610367]
12. Gerard M, Deleersnijder A, Demeulemeester J, Debyser Z, Baekelandt V. Unraveling the role of peptidyl-prolyl isomerases in neurodegeneration. Mol Neurobiol. 2011; 44:13–27. [PubMed: 21553017]
13. Dorner M, Horwitz JA, Donovan BM, Labitt RN, Budell WC, Friling T, Vogt A, Catanese MT, Satoh T, Kawai T, Akira S, Law M, Rice CM, Ploss A. Completion of the entire hepatitis C virus life cycle in genetically humanized mice. Nature. 2013; 501:237–241. [PubMed: 23903655]
14. Coelmont L, Hanoulle X, Chatterji U, Berger C, Snoeck J, Bobardt M, Lim P, Vliegen I, Paeshuyse J, Vuagniaux G, Vandamme AM, Bartenschlager R, Gallay P, Lippens G, Neyts J. DEB025 (Alisporivir) inhibits hepatitis C virus replication by preventing a cyclophilin A induced cis-trans isomerisation in domain II of NS5A. PLoS One. 2010; 5:e13687. [PubMed: 21060866]
15. Schaller T, Ocwieja KE, Rasaiyaah J, Price AJ, Brady TL, Roth SL, Hue S, Fletcher AJ, Lee K, KewalRamani VN, Noursadeghi M, Jenner RG, James LC, Bushman FD, Towers GJ. HIV-1 capsid-cyclophilin interactions determine nuclear import pathway, integration targeting and replication efficiency. PLoS Path. 2011; 7:e1002439.
16. Franke EK, Luban J. Inhibition of HIV-1 replication by cyclosporine A or related compounds correlates with the ability to disrupt the Gag-cyclophilin A interaction. Virology. 1996; 222:279–282. [PubMed: 8806510]
17. Rasaiyaah J, Tan CP, Fletcher AJ, Price AJ, Blondeau C, Hilditch L, Jacques DA, Selwood DL, James LC, Noursadeghi M, Towers GJ. HIV-1 evades innate immune recognition through specific cofactor recruitment. Nature. 2013; 503:402–405. [PubMed: 24196705]
18. Lin K, Gallay P. Curing a viral infection by targeting the host: the example of cyclophilin inhibitors. Antiviral Res. 2013; 99:68–77. [PubMed: 23578729]
19. Schneuwly S, Shortridge RD, Larrivee DC, Ono T, Ozaki M, Pak WL. Drosophila ninaA gene encodes an eye-specific cyclophilin (cyclosporine A binding protein). Proc Natl Acad Sci U S A. 1989; 86:5390–5394. [PubMed: 2664782]
20. Shieh BH, Stamnes MA, Seavello S, Harris GL, Zuker CS. The ninaA gene required for visual transduction in Drosophila encodes a homologue of cyclosporin A-binding protein. Nature. 1989; 338:67–70. [PubMed: 2493138]
21. Baker EK, Colley NJ, Zuker CS. The cyclophilin homolog NinaA functions as a chaperone, forming a stable complex in vivo with its protein target rhodopsin. EMBO J. 1994; 13:4886–4895. [PubMed: 7957056]
22. Ingelfinger D, Gothel SF, Marahiel MA, Reidt U, Ficner R, Luhrmann R, Achsel T. Two protein-protein interaction sites on the spliceosome-associated human cyclophilin CypH. Nucleic Acids Res. 2003; 31:4791–4796. [PubMed: 12907720]
23. Xu C, Zhang J, Huang X, Sun J, Xu Y, Tang Y, Wu J, Shi Y, Huang Q, Zhang Q. Solution structure of human peptidyl prolyl isomerase-like protein 1 and insights into its interaction with SKIP. J Biol Chem. 2006; 281:15900–15908. [PubMed: 16595688]
24. Reidt U, Wahl MC, Fasshauer D, Horowitz DS, Luhrmann R, Ficner R. Crystal structure of a complex between human spliceosomal cyclophilin H and a U4/U6 snRNP-60K peptide. J Mol Biol. 2003; 331:45–56. [PubMed: 12875835]
25. Ishikawa Y, Vranka JA, Boudko SP, Pokidysheva E, Mizuno K, Zientek K, Keene DR, Rashmir-Raven AM, Nagata K, Winand NJ, Bachinger HP. Mutation in cyclophilin B that causes hyperelastosis cutis in American Quarter Horse does not affect peptidylprolyl cis-trans isomerase

activity but shows altered cyclophilin B-protein interactions and affects collagen folding. J Biol Chem. 2012; 287:22253–22265. [PubMed: 22556420]

26. Cho KI, Patil H, Senda E, Wang J, Yi H, Qiu S, Yoon D, Yu M, Orry A, Peachey NS, Ferreira PA. Differential Loss of Prolyl Isomerase or Chaperone Activity of Ran-binding Protein 2 (Ranbp2) Unveils Distinct Physiological Roles of Its Cyclophilin Domain in Proteostasis. J Biol Chem. 2014; 289:4600–4625. [PubMed: 24403063]
27. Wu J, Matunis MJ, Kraemer D, Blobel G, Coutavas E. Nup358, a cytoplasmically exposed nucleoporin with peptide repeats, Ran-GTP binding sites, zinc fingers, a cyclophilin A homologous domain, and a leucine-rich region. J Biol Chem. 1995; 270:14209–14213. [PubMed: 7775481]
28. Yokoyama N, Hayashi N, Seki T, Pante N, Ohba T, Nishii K, Kuma K, Hayashida T, Miyata T, Aebi U, et al. A giant nucleopore protein that binds Ran/TC4. Nature. 1995; 376:184–188. [PubMed: 7603572]
29. Ferreira PA, Hom JT, Pak WL. Retina-specifically expressed novel subtypes of bovine cyclophilin. J Biol Chem. 1995; 270:23179–23188. [PubMed: 7559465]
30. Mavlyutov TA, Cai Y, Ferreira PA. Identification of RanBP2- and Kinesin-Mediated Transport Pathways with Restricted Neuronal and Subcellular Localization. Traffic. 2002; 3:630–640. [PubMed: 12191015]
31. Delphin C, Guan T, Melchior F, Gerace L. RanGTP targets p97 to RanBP2, a filamentous protein localized at the cytoplasmic periphery of the nuclear pore complex. Mol Biol Cell. 1997; 8:2379–2390. [PubMed: 9398662]
32. Vetter IR, Nowak C, Nishimoto T, Kuhlmann J, Wittinghofer A. Structure of a Ran-binding domain complexed with Ran bound to a GTP analogue: implications for nuclear transport. Nature. 1999; 398:39–46. [PubMed: 10078529]
33. Hamada M, Haeger A, Jeganathan KB, van Ree JH, Malureanu L, Walde S, Joseph J, Kehlenbach RH, van Deursen JM. Ran-dependent docking of importin-beta to RanBP2/Nup358 filaments is essential for protein import and cell viability. J Cell Biol. 2011; 194:597–612. [PubMed: 21859863]
34. Walde S, Thakar K, Hutten S, Spillner C, Nath A, Rothbauer U, Wiemann S, Kehlenbach RH. The nucleoporin Nup358/RanBP2 promotes nuclear import in a cargo- and transport receptor-specific manner. Traffic. 2012; 13:218–233. [PubMed: 21995724]
35. Packham S, Warsito D, Lin Y, Sadi S, Karlsson R, Sehat B, Larsson O. Nuclear translocation of IGF-1R via p150(Glued) and an importin-beta/RanBP2-dependent pathway in cancer cells. Oncogene. 2015; 34:2227–2238. [PubMed: 24909165]
36. Frohnert C, Hutten S, Walde S, Nath A, Kehlenbach RH. Importin 7 and Nup358 promote nuclear import of the protein component of human telomerase. PLoS One. 2014; 9:e88887. [PubMed: 24586428]
37. Singh BB, Patel HH, Roepman R, Schick D, Ferreira PA. The zinc finger cluster domain of RanBP2 is a specific docking site for the nuclear export factor, exportin-1. J Biol Chem. 1999; 274:37370–37378. [PubMed: 10601307]
38. Werner A, Flotho A, Melchior F. The RanBP2/RanGAP1(*)SUMO1/Ubc9 Complex Is a Multisubunit SUMO E3 Ligase. Mol Cell. 2012; 46:287–298. [PubMed: 22464730]
39. Pichler A, Gast A, Seeler JS, Dejean A, Melchior F. The nucleoporin RanBP2 has SUMO1 E3 ligase activity. Cell. 2002; 108:109–120. [PubMed: 11792325]
40. Saitoh H, Sparrow DB, Shiomi T, Pu RT, Nishimoto T, Mohun TJ, Dasso M. Ubc9p and the conjugation of SUMO-1 to RanGAP1 and RanBP2. Curr Biol. 1998; 8:121–124. [PubMed: 9427648]
41. Cai Y, Singh BB, Aslanukov A, Zhao H, Ferreira PA. The docking of kinesins, KIF5B and KIF5C, to Ran-binding protein 2 (RanBP2) is mediated via a novel RanBP2 domain. J Biol Chem. 2001; 276:41594–41602. [PubMed: 11553612]
42. Cho KI, Cai Y, Yi H, Yeh A, Aslanukov A, Ferreira PA. Association of the Kinesin-Binding Domain of RanBP2 to KIF5B and KIF5C Determines Mitochondria Localization and Function. Traffic. 2007; 8:1722–1735. [PubMed: 17887960]

43. Cho KI, Yi H, Desai R, Hand AR, Haas AL, Ferreira PA. RANBP2 is an allosteric activator of the conventional kinesin-1 motor protein, KIF5B, in a minimal cell-free system. EMBO reports. 2009; 10:480–486. [PubMed: 19305391]
44. Ferreira PA, Nakayama TA, Pak WL, Travis GH. Cyclophilin-related protein RanBP2 acts as chaperone for red/green opsin. Nature. 1996; 383:637–640. [PubMed: 8857542]
45. Ferreira PA, Nakayama TA, Travis GH. Interconversion of red opsin isoforms by the cyclophilin-related chaperone protein Ran-binding protein 2. Proc Natl Acad Sci U S A. 1997; 94:1556–1561. [PubMed: 9037092]
46. Yi H, Friedman JL, Ferreira PA. The cyclophilin-like domain of Ran-binding protein-2 modulates selectively the activity of the ubiquitin-proteasome system and protein biogenesis. J Biol Chem. 2007; 282:34770–34778. [PubMed: 17911097]
47. Ferreira PA, Yunfei C, Schick D, Roepman R. The cyclophilin-like domain mediates the association of Ran-binding protein 2 with subunits of the 19 S regulatory complex of the proteasome. J Biol Chem. 1998; 273:24676–24682. [PubMed: 9733766]
48. Miklossy G, Hilliard TS, Turkson J. Therapeutic modulators of STAT signalling for human diseases. Nat Rev Drug Discov. 2013; 12:611–629. [PubMed: 23903221]
49. O'Shea JJ, Holland SM, Staudt LM. JAKs and STATs in immunity, immunodeficiency, and cancer. N Engl J Med. 2013; 368:161–170. [PubMed: 23301733]
50. Yu H, Pardoll D, Jove R. STATs in cancer inflammation and immunity: a leading role for STAT3. Nat Rev Cancer. 2009; 9:798–809. [PubMed: 19851315]
51. Burda JE, Sofroniew MV. Reactive gliosis and the multicellular response to CNS damage and disease. Neuron. 2014; 81:229–248. [PubMed: 24462092]
52. Samardzija M, Wenzel A, Aufenberg S, Thiersch M, Reme C, Grimm C. Differential role of Jak-STAT signaling in retinal degenerations. FASEB J. 2006; 20:2411–2413. [PubMed: 16966486]
53. Schaeferhoff K, Michalakis S, Tanimoto N, Fischer MD, Becirovic E, Beck SC, Huber G, Rieger N, Riess O, Wissinger B, Biel M, Seeliger MW, Bonin M. Induction of STAT3-related genes in fast degenerating cone photoreceptors of cpfl1 mice. Cell Mol Life Sci. 2010; 67:3173–3186. [PubMed: 20467778]
54. Ozawa Y, Nakao K, Kurihara T, Shimazaki T, Shimmura S, Ishida S, Yoshimura A, Tsubota K, Okano H. Roles of STAT3/SOCS3 pathway in regulating the visual function and ubiquitin-proteasome-dependent degradation of rhodopsin during retinal inflammation. J Biol Chem. 2008; 283:24561–24570. [PubMed: 18614536]
55. Jiang K, Wright KL, Zhu P, Szego MJ, Bramall AN, Hauswirth WW, Li Q, Egan SE, McInnes RR. STAT3 promotes survival of mutant photoreceptors in inherited photoreceptor degeneration models. Proc Natl Acad Sci U S A. 2014; 111:E5716–5723. [PubMed: 25512545]
56. Kim HJ, Kim NC, Wang YD, Scarborough EA, Moore J, Diaz Z, MacLea KS, Freibaum B, Li S, Molliex A, Kanagaraj AP, Carter R, Boylan KB, Wojtas AM, Rademakers R, Pinkus JL, Greenberg SA, Trojanowski JQ, Traynor BJ, Smith BN, Topp S, Gkazi AS, Miller J, Shaw CE, Kottlors M, Kirschner J, Pestronk A, Li YR, Ford AF, Gitler AD, Benatar M, King OD, Kimonis VE, Ross ED, Weihl CC, Shorter J, Taylor JP. Mutations in prion-like domains in hnRNPA2B1 and hnRNPA1 cause multisystem proteinopathy and ALS. Nature. 2013; 495:467–473. [PubMed: 23455423]
57. Gardner JC, Webb TR, Kanuga N, Robson AG, Holder GE, Stockman A, Ripamonti C, Ebenezer ND, Ogun O, Devery S, Wright GA, Maher ER, Cheetham ME, Moore AT, Michaelides M, Hardcastle AJ. X-linked cone dystrophy caused by mutation of the red and green cone opsins. Am J Hum Genet. 2010; 87:26–39. [PubMed: 20579627]
58. Bichel K, Price AJ, Schaller T, Towers GJ, Freund SM, James LC. HIV-1 capsid undergoes coupled binding and isomerization by the nuclear pore protein NUP358. Retrovirology. 2013; 10:81. [PubMed: 23902822]
59. Fraser JS, Clarkson MW, Degnan SC, Erion R, Kern D, Alber T. Hidden alternative structures of proline isomerase essential for catalysis. Nature. 2009; 462:669–673. [PubMed: 19956261]
60. Ramanathan A, Savol AJ, Langmead CJ, Agarwal PK, Chennubhotla CS. Discovering conformational sub-states relevant to protein function. PLoS One. 2011; 6:e15827. [PubMed: 21297978]

61. Burnley BT, Afonine PV, Adams PD, Gros P. Modelling dynamics in protein crystal structures by ensemble refinement. Elife. 2012; 1:e00311. [PubMed: 23251785]
62. Liu J, Chen CM, Walsh CT. Human and Escherichia coli cyclophilins: sensitivity to inhibition by the immunosuppressant cyclosporin A correlates with a specific tryptophan residue. Biochemistry (Mosc). 1991; 30:2306–2310.
63. Hoffmann K, Kakalis LT, Anderson KS, Armitage IM, Handschumacher RE. Expression of human cyclophilin-40 and the effect of the His141-->Trp mutation on catalysis and cyclosporin A binding. Eur J Biochem. 1995; 229:188–193. [PubMed: 7744028]
64. Lin DH, Zimmermann S, Stuwe T, Stuwe E, Hoelz A. Structural and functional analysis of the C-terminal domain of Nup358/RanBP2. J Mol Biol. 2013; 425:1318–1329. [PubMed: 23353830]
65. Lammers M, Neumann H, Chin JW, James LC. Acetylation regulates cyclophilin A catalysis, immunosuppression and HIV isomerization. Nat Chem Biol. 2010; 6:331–337. [PubMed: 20364129]
66. Ke H. Similarities and differences between human cyclophilin A and other beta-barrel structures. Structural refinement at 1.63 A resolution. J Mol Biol. 1992; 228:539–550. [PubMed: 1453463]
67. Bauer K, Kretzschmar AK, Cvijic H, Blumert C, Loffler D, Brocke-Heidrich K, Schiene-Fischer C, Fischer G, Sinz A, Clevenger CV, Horn F. Cyclophilins contribute to Stat3 signaling and survival of multiple myeloma cells. Oncogene. 2009; 28:2784–2795. [PubMed: 19503092]
68. al-Ubaidi MR, Font RL, Quiambao AB, Keener MJ, Liou GI, Overbeek PA, Baehr W. Bilateral retinal and brain tumors in transgenic mice expressing simian virus 40 large T antigen under control of the human interphotoreceptor retinoid-binding protein promoter. J Cell Biol. 1992; 119:1681–1687. [PubMed: 1334963]
69. Tan E, Ding XQ, Saadi A, Agarwal N, Naash MI, Al-Ubaidi MR. Expression of cone-photoreceptor-specific antigens in a cell line derived from retinal tumors in transgenic mice. Invest Ophthalmol Vis Sci. 2004; 45:764–768. [PubMed: 14985288]
70. Mikol V, Kallen J, Pflugl G, Walkinshaw MD. X-ray structure of a monomeric cyclophilin A-cyclosporin A crystal complex at 2.1 A resolution. J Mol Biol. 1993; 234:1119–1130. [PubMed: 8263916]
71. Xia X, Li Y, Huang D, Wang Z, Luo L, Song Y, Zhao L, Wen R. Oncostatin M protects rod and cone photoreceptors and promotes regeneration of cone outer segment in a rat model of retinal degeneration. PLoS One. 2011; 6:e18282. [PubMed: 21479182]
72. Noorwez SM, Kuksa V, Imanishi Y, Zhu L, Filipek S, Palczewski K, Kaushal S. Pharmacological chaperone-mediated in vivo folding and stabilization of the P23H-opsin mutant associated with autosomal dominant retinitis pigmentosa. J Biol Chem. 2003; 278:14442–14450. [PubMed: 12566452]
73. Deng J, Chen S, Wang F, Zhao H, Xie Z, Xu Z, Zhang Q, Liang P, Zhai X, Cheng Y. Effects of hnRNP A2/B1 Knockdown on Inhibition of Glioblastoma Cell Invasion, Growth and Survival. Mol Neurobiol. 2015
74. Golan-Gerstl R, Cohen M, Shilo A, Suh SS, Bakacs A, Coppola L, Karni R. Splicing factor hnRNP A2/B1 regulates tumor suppressor gene splicing and is an oncogenic driver in glioblastoma. Cancer Res. 2011; 71:4464–4472. [PubMed: 21586613]
75. Arkin MR, Tang Y, Wells JA. Small-molecule inhibitors of protein-protein interactions: progressing toward the reality. Chem Biol. 2014; 21:1102–1114. [PubMed: 25237857]
76. Linderstrøm-Lang, K.; Schellman, JA. Protein structure and enzyme activity. In: Boyer, PD.; Lardy, H.; Myrback, K., editors. The Enzymes. 2. Academic Press; 1959. p. 443-510.
77. Monod J, Wyman J, Changeux JP. On the Nature of Allosteric Transitions: A Plausible Model. J Mol Biol. 1965; 12:88–118. [PubMed: 14343300]
78. Volkman BF, Lipson D, Wemmer DE, Kern D. Two-state allosteric behavior in a single-domain signaling protein. Science. 2001; 291:2429–2433. [PubMed: 11264542]
79. Tsai CJ, Del Sol A, Nussinov R. Protein allostery, signal transmission and dynamics: a classification scheme of allosteric mechanisms. Mol Biosyst. 2009; 5:207–216. [PubMed: 19225609]

80. Li P, Martins IR, Amarasinghe GK, Rosen MK. Internal dynamics control activation and activity of the autoinhibited Vav DH domain. Nat Struct Mol Biol. 2008; 15:613–618. [PubMed: 18488041]

81. Abagyan R, Totrov M. Biased probability Monte Carlo conformational searches and electrostatic calculations for peptides and proteins. J Mol Biol. 1994; 235:983–1002. [PubMed: 8289329]

82. Abagyan R, Totrov M, Kuznetsov D. ICM-a new method for protein modeling and design: applications to docking and structure prediction from the distorted native conformation. J Comput Chem. 1994; 15:488–506.

83. Orry AJ, Abagyan R. Preparation and refinement of model protein-ligand complexes. Methods Mol Biol. 2012; 857:351–373. [PubMed: 22323230]

84. Lipinski CA, Lombardo F, Dominy BW, Feeney PJ. Experimental and computational approaches to estimate solubility and permeability in drug discovery and development settings. Adv Drug Deliv Rev. 2001; 46:3–26. [PubMed: 11259830]

85. Totrov, M.; Abagyan, R. Derivation of sensitive discrimination potential for virtual ligand screening. Third Annual International Conference on Computational Molecular Biology; Lyon, France: Association for Computing Machinery; 1999. p. 312-320.

86. Baell JB, Holloway GA. New substructure filters for removal of pan assay interference compounds (PAINS) from screening libraries and for their exclusion in bioassays. J Med Chem. 2010; 53:2719–2740. [PubMed: 20131845]

87. Totrov M. Atomic property fields: generalized 3D pharmacophoric potential for automated ligand superposition, pharmacophore elucidation and 3D QSAR. Chem Biol Drug Des. 2008; 71:15–27. [PubMed: 18069986]

88. Ferreira PA. Characterization of RanBP2-associated molecular components in neuroretina. Methods Enzymol. 2000; 315:455–468. [PubMed: 10736720]

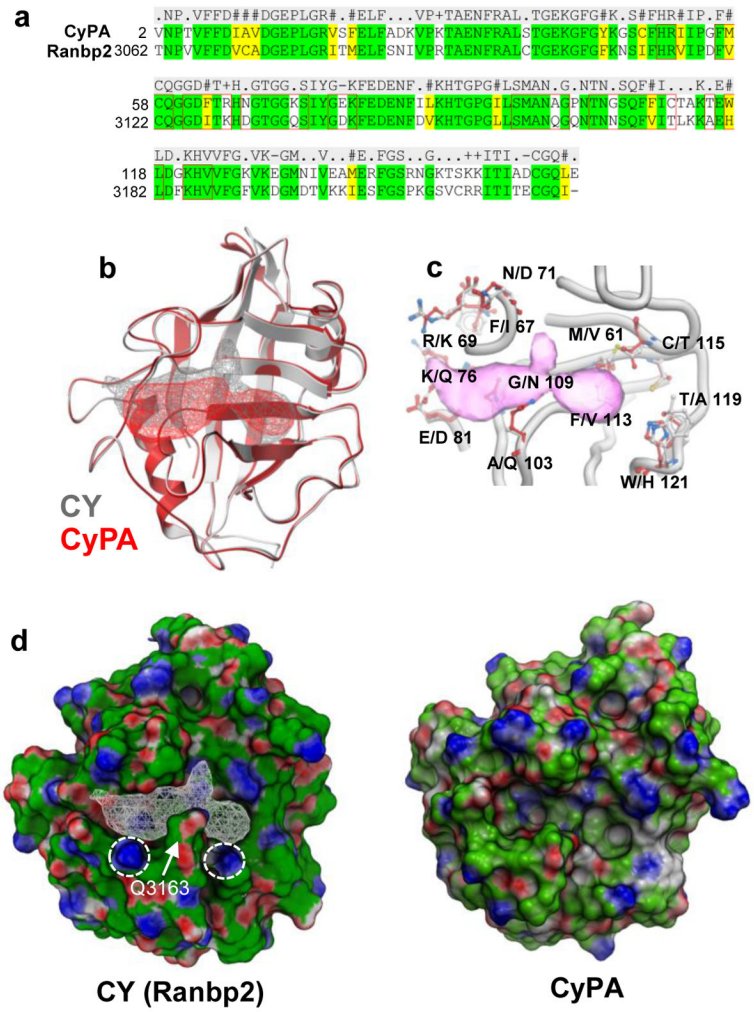

FIGURE 1. Heterogeneity of structural ensembles between the PPIase pockets of CY of Ranbp2 and CyPA

(a) Amino acid sequence alignment of CY of Ranbp2 and cyclophilin A (CyPA). CY and CyPA are 65% identical. Residues within 7Å of the PPIase pocket are noted within red line boxes. (b) Ribbon representation of superposition of CY of Ranbp2 (gray) and CyPA (red). Mesh represents extended PPIase pocket of CY (gray) and that of CyPA (red). (c) Non-conserved residues of the PPIase/CsA-binding pockets of CyPA (listed first) and CY of Ranbp2 (listed second). Extended CY PPIase pocket is in pink. Numbering refers CyPA residues. (d) Surface representations of CY of Ranbp2 and CyPA colored by qualitative electrostatic potential calculated by ICM using a color scale from red to blue and values of +/−5 kcal/electron units (+5=blue, −5=red). The conserved K3142 and K3185 (circles) and the nonconserved Q3163 residues of CY (arrow) and its PPIase pocket (white mesh) are shown. Variable orientations of side chains of K3142 and K3185 of CY of Ranbp2 and equivalent residues in CyPA cause surface electrostatic shifts.

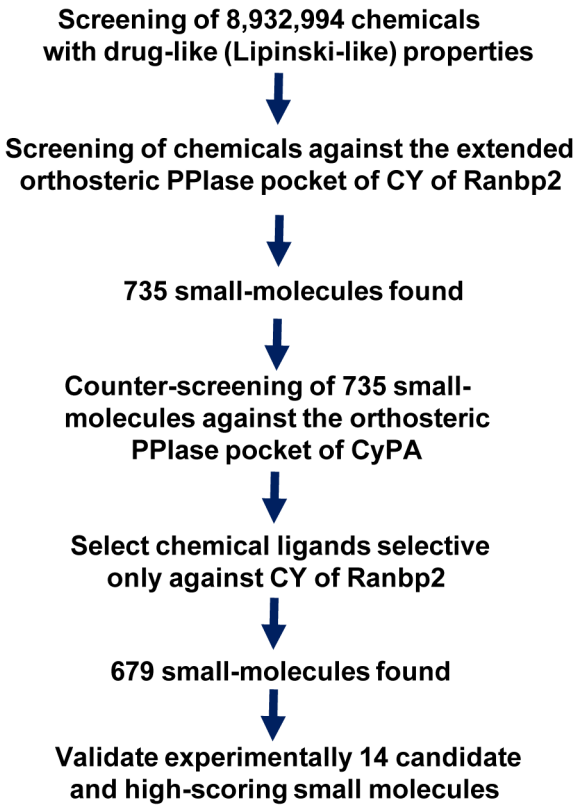

FIGURE 2.

Diagram of strategy for structure-based ligand screening *in silico* of candidate small molecules against the PPIase pocket of CY of Ranbp2.

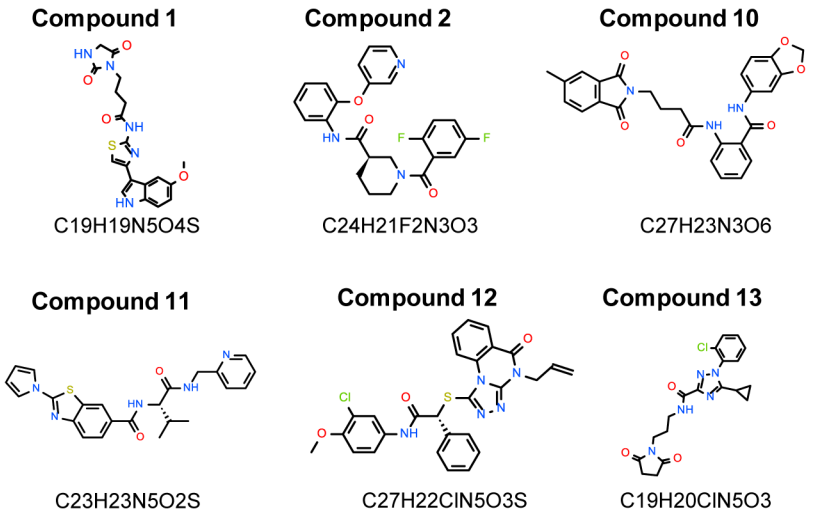

FIGURE 3. Chemical structures of bioactive ligands of CY PPIase pocket identified by *in silico* screening and examined by this study experimentally

Compound 1, 4-(2,5-Dioxo-imidazolidin-1-yl)-N-[4-(5-methoxy-1H-indol-3-yl)-thiazol-2-yl]-butyramide; compound 2, 1-(2,5-difluorobenzoyl)-N-[2-(3-pyridinyloxy)phenyl]-3-piperidinecarboxamide; compound 10, N-(2H-1,3-benzodioxol-5-yl)-2-[4-(5-methyl-1,3-dioxo-2,3-dihydro-1H-isoindol-2-yl)butanamido]benzamide; compound 11, (S)-N-(3-methyl-1-oxo-1-((pyridin-2-ylmethyl)amino)butan-2-yl)-2-(1H-pyrrol-1-yl)benzodthiazole-6-carboxamide; compound 12, N-(3-chloro-4-methoxyphenyl)-2-{[5-oxo-4-(prop-2-en-1-yl)-4H,5H-[1,2,4]triazolo[4,3-a]quinazolin-1-yl]sulfanyl}-2-phenylacetamide; compound 13, 1-(2-chlorophenyl)-5-cyclopropyl-N-[3-(2,5-dioxopyrrolidin-1-yl)propyl]-1H-1,2,4-triazole-3-carboxamide.

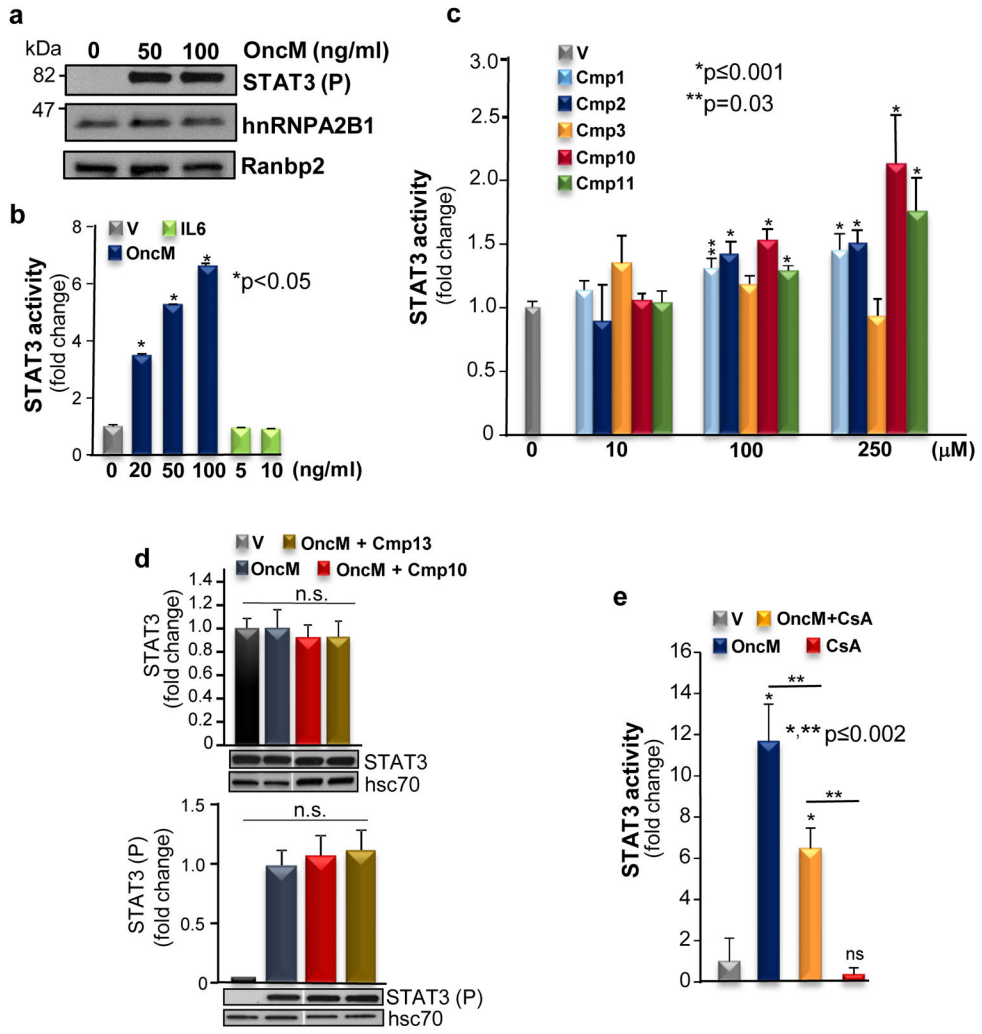

FIGURE 4. Pharmacological properties of CY chemical ligands in STAT3 transcriptional activation potential

(a) Immunoblots of STAT3(P) (activated STAT3) from homogenates of STAT3 luciferase reporter HeLa stable cell line treated or untreated with oncostatin M (OncM). Levels of hnRNPA2B1 and Ranbp2 levels remain unchanged between OncM untreated and treated cells. (b) Luciferase activity induced by STAT3-transcriptional activation in the absence or presence of OncM and IL-6. (c) Dose-dependent responses of STAT3-transcriptional activity of STAT3 luciferase reporter HeLa stable cells treated with OncM in the absence and presence of small molecules (Cmp). (d) Levels of latent STAT3 and activated STAT3(P) remain unchanged in the absence or presence of small molecules with (e.g. Cmp 10) and without effect (e.g. Cmp 13) on OncM-stimulated STAT3 activity. (e) CsA suppresses the STAT3-transcriptional activity stimulated by OncM. Data shown represent the mean ± s.d., *n* =3 (b, c, d, e); *n.s.*, non-significant. Legend: V, vehicle; Cmp, compound (small molecule).

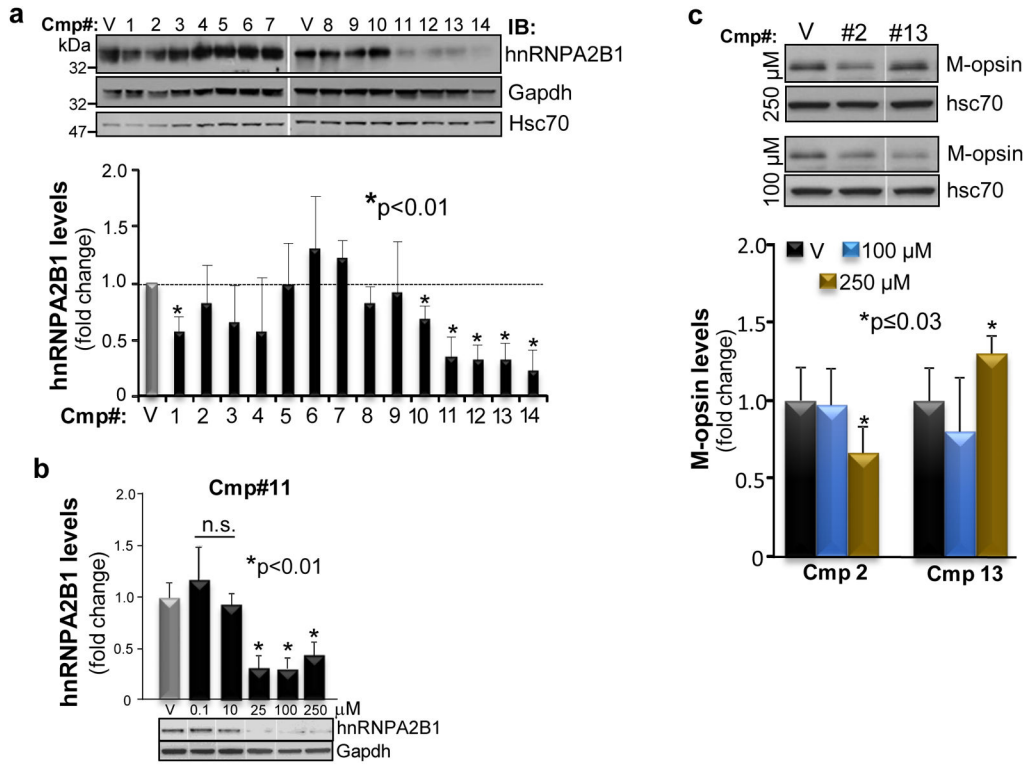

FIGURE 5. Pharmacological effects of CY chemical ligands in hnRNPA2B1 and M-opsin proteostasis

(a) Immunoblot (top panel) and quantitative analyses (lower panel) of hnRNPA2B1 levels in homogenates of STAT3 luciferase reporter HeLa stable cells untreated and treated with small molecules (100 µM). Compounds 11–13 reduce strongly hnRNPA2B1 levels. Compound 14 is cytotoxic. (b) Quantitative analyses (upper graph) by immunoblot of hnRNPA2B1 levels (lower panel) in homogenates of HeLa cells untreated and treated with increasing concentrations of compound 11. (c) Immunoblot (upper panel) and quantitative analyses (lower panel) of M-opsin levels in homogenates of 661W cells untreated and treated with small molecules. Compounds 2 and 13 reduce and increase M-opsin levels, respectively. Data shown represent the mean ± s.d., $n = 4$ (a–c). Legend: V, vehicle (compound solvent) only; Cmp, compound (small molecule); Gapdh, Glyceraldehyde 3-phosphate dehydrogenase; hsc70, cytosolic heat shock cognate protein 70.

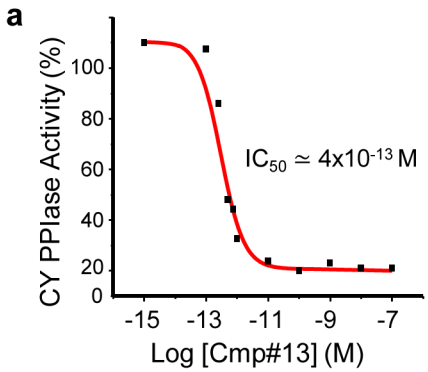

b

	k_{cat}/K_m ($mM^{-1}s^{-1}$)
CyPA	1544.6 ± 229.4
CyPA + CsA	20.6 ± 21.0
CyPA + Cmp13	1694.0 ± 370.4
CY	142.9 ± 43.3
CY + CsA	148.3 ± 60.1
CY + Cmp13	25.5 ± 8.6

FIGURE 6. Inhibitory effects of compound 13 and CsA on CY and CyPA PPIase activities

(a) Direct inhibition of PPIase activity of CY by compound 13. Compound 13 has an IC_{50} of $\simeq 4\times10^{-13}$ M on the catalytic efficiency (k_{cat}/K_m) of CY. (b) Inhibitory effects of CsA and compound 13 on the catalytic efficiencies of CyPA and CY of Ranbp2. Data shown represent the mean ± s.d., n =4–6 (b). Legend: V, vehicle; Cmp, compound (small molecule).

a

CY (Ranbp2)	CyPA	CY + Cmp1	CY + Cmp2	CY + Cmp10	CY + Cmp11	CY + Cmp12	CY + Cmp13	CyPA + CsA
H3114	H54	0.00	14.04	4.11	10.96	13.72	9.43	0.00
R3115	R55	24.39	30.64	36.88	35.91	25.12	36.76	41.24
I3117	I57	0.00	0.00	0.00	0.00	0.00	0.00	2.20
F3120	F60	16.64	11.31	21.63	11.59	0.32	20.39	38.83
V3121	M61	0.00	4.10	0.00	6.93	0.00	1.89	9.82
Q3123	Q63	16.07	24.32	21.05	24.39	16.17	25.68	20.59
D3131	N71	0.00	0.00	2.40	0.48	11.18	0.00	0.00
G3132	G72	15.13	19.10	25.28	21.93	25.35	17.62	18.16
T3133	T73	25.70	2.52	11.17	17.52	24.95	13.39	7.77
G3134	G74	5.00	2.62	11.17	15.04	12.75	4.04	0.00
G3135	G75	0.00	0.00	0.00	6.02	0.24	0.00	0.00
D3141	E81	0.00	0.00	0.00	10.43	0.00	0.00	0.00
K3142	K82	0.00	0.00	0.63	8.48	0.00	0.00	0.00
M3160	M100	0.00	0.00	0.00	0.00	0.80	0.00	0.00
A3161	A101	20.51	21.00	16.55	25.14	21.92	23.17	18.64
N3162	N102	16.07	21.00	11.17	13.43	15.67	13.31	33.97
Q3163	A103	43.80	51.94	43.06	34.74	58.89	36.76	19.96
N3169	G109	17.85	7.14	16.55	28.62	24.23	14.73	0.00
Q3171	Q111	20.30	23.90	22.85	25.00	25.23	24.31	13.16
V3173	F113	1.89	7.85	0.00	13.83	9.11	8.48	19.57
H3181	W121	0.00	0.00	20.33	0.00	0.00	11.65	25.83
L3182	L122	10.33	5.96	11.17	7.20	10.02	14.08	19.88
K3185	K125	5.66	14.05	13.34	0.00	14.83	7.38	0.00
H3186	H126	19.36	19.07	16.85	11.92	23.29	17.59	19.92

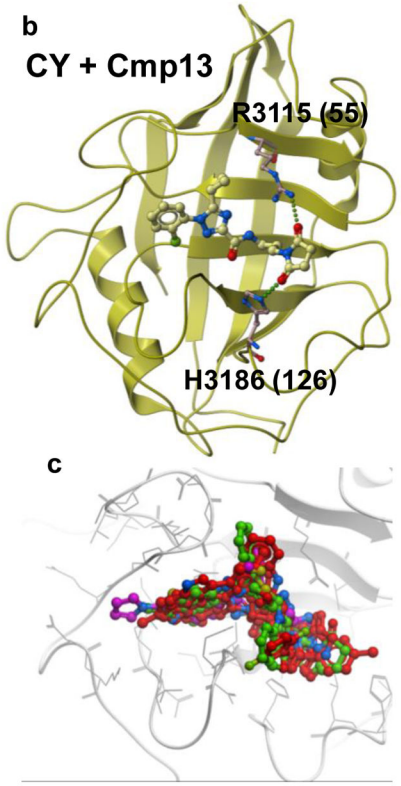

FIGURE 7. Structural poses of CY-ligand complexes

(a) Surface contact areas (Å^2) between docked ligands of CY and residues of PPIase pocket of CY determined by molecular modeling with ICM. Counterpart residues in CyPA are also shown (2nd column). Non-conserved residues in CY are shown in bold. Contact areas (Å^2) between docked CsA and residues of PPIase pocket of CyPA as determined by X-ray crystallography are shown (last column). Numbers in red denote residues establishing interactions with chemical probes identified by this study and that are known not to participate in interactions between CyPA and CsA. Residues in bold are unique to CY of Ranbp2. Residues in green establish hydrogen bonds with compound 13. (b) Hydrogen bonding between compound 13 and the conserved residues, R3115 and H3186, of the PPIase pocket of CY. Numbers in parenthesis are counterpart residues in CyPA. (c) Superposition of ligands of PPIase pocket of CY; compound 11 (purple) protrudes out the PPIase pocket of CY.